SCIREA Journal of Civil Engineering and Building Construction
http://www.scirea.org/journal/CEBC
July 4, 2023
Volume 8, Issue 2, April 2023
https://doi.org/10.54647/cebc560120

The use of the S-transform in *Prazeres* clay site characterization combining in situ and laboratory tests

Jorge Machado de Carvalho[1*], Mafalda Lopes Laranjo[2]

[1] CERENA-FEUP, Department of Mining Engineering, Faculty of Engineering, University of Porto, Portugal, jorcarv@fe.up.pt

[2] PROMETHEUS, Instituto Politécnico de Viana do Castelo, Portugal, mlopes@estg.ipvc.pt

[*] Corresponding author, e-mail: jorcarv@fe.up.pt

Abstract

In the framework of a research project led by the Faculty of Engineering - University of Porto (FEUP), an investigation and characterization campaign was carried out on a profile of the Lisbon *Prazeres* clay and limestone formation. The campaign comprised the use of in situ P and S-waves seismic cross-hole (CH) tests, using a borehole hammer and a sparker source, as well as mechanical tests such as SPT, PMT and SBPT. In addition, laboratory tests were carried out on undisturbed samples, using bender and ultrasonic transducers prior and during triaxial tests. The fact that two different in situ seismic sources were used allowed a comparative seismic signal analysis in time, frequency and time-frequency domains, using the Short Time Fourier Transform, STFT, and the S-Transform, ST. Following a summarized description of the developed work and obtained direct and indirect results, this paper addresses the analysis and comparison of the referred CH results using the STFT and ST approach.

Keywords: *Prazeres* Miocene clays, bender and ultrasonic transducers, seismic cross-hole, S-Transform

1 Introduction

Miocene clays form a significant part of Lisbon subsoil, where several relevant construction works have been built in the last decades. These works required detailed ground information, comprising in situ and laboratory tests concerning different geotechnical layers. Included on a research program these data were gathered in order to establish trends on the geotechnical properties of Miocene clays. The research program included tests on an experimental site, located at Av. Visconde Valmor in Lisbon. In this experimental site, a set of in situ tests was performed, including SPT in one borehole at 1.5 m spacing, Ménard Pressuremeter Test (PMT) at four depths in a different borehole, Self-boring Pressuremeter Test (SBPT) at three depths in a third hole. A fourth hole was opened to allow the performance of CH seismic tests conducted in two stages using different seismic sources. Two cubic block samples were also collected at 4 m depth and taken to the Geotechnical Laboratory at Faculty of Engineering University of Porto (FEUP), where laboratory tests, including triaxial and oedometric tests were performed. Prior to the mechanical testing, S-wave measurements were made using bender and ultrasonic transducers. These measurements were made prior to the placement on the triaxial chambers, and in some cases, during compression at different extension rates.

2 Objective

The objective of this work is to characterize strain stiffness of *Prazeres* clay and limestones formation, by means of seismic wave velocity measurements, comparing the results of CH seismic tests performed on the experimental site and laboratory measurements of S-wave velocities on samples from the experimental site collected from a block.

The effect of the energy impact in seismic CH tests is discussed by analyzing the results from two sets of tests: the first using a sparker source, and the second using a mechanical bidirectional hammer. A comparison of the results of cross-hole and other in situ tests, such as PMT and SBPT along the same soil profile is addressed. Although SBPT minimizes the disturbance of the surrounding soil caused by probe installation, there are differences in the mechanical parameters obtained using SBPT and CH seismic tests, associated to distinct

induced strain levels, with consequent implications on very small strain stiffness shear modulus (G_0). The influence of strain level on shear modulus is discussed.

3 Geological background

The Lower Tagus basin is located in the western margin of the Iberian plate. Its geological history is very complex and derives from the interaction between tectonic events and variations on the sea level. The basin was formed in the beginning of the Tertiary when the region sank between faults and was filled with detrital sediments from peripheral areas. This sedimentation is believed to be a continuous phenomenon that is still active [1]. The Miocene Series, which results from about 16 million years of sedimentation, is around 300 m thick and comprises several geological formations that include hard soils and soft rocks. In this paper only *Prazeres* clay, one of the main clayey formation, was addressed. *Prazeres* clay forms the base of the Miocene Series and includes argillites, silty argillites, silts, clayey silts, silty clays, clays, marly argillites, marls and limes [2]. Geologically it is a very heterogeneous formation. Plasticity is medium, with water content close to the plastic limit, thus consistency indexes typical of stiff or very stiff soils. This formation occupies an important part of Lisbon subsoil, including areas of historical interest, as shown in Lisbon Geological Chart, [3].

4 In situ investigation

4.1 Geophysical survey

The main objective was to obtain reliable in situ elastic moduli measurements, in particular shear modulus, G_0, and Poisson's ratio, derived from P and S-wave velocity profiles and evaluating the hypothetical clay anisotropic stress state based on S waves propagated horizontally and polarized vertically (S_{hv}) and S waves propagated and polarized horizontally (S_{hh}) velocities. In addition, the use of different equipment in different seasons, allowed comparing both results in time and frequency domains.

Field equipment comprised the two following systems: a) a Soil Dynamics mechanical bidirectional vertical hammer and a Geo-Stuff BHG-3 14 Hz triaxial geophone system, coupled to a Geometrics Smartseis 12 channel seismograph and b) a Geotomographie electrical sparker source, SH-66 for SH-waves and a Geotomographie BGK3 14 Hz triaxial geophone system coupled to a Seistronix Ras- 12 channel seismograph.

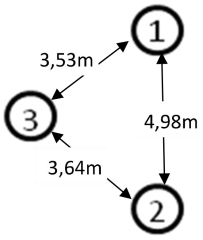

Fig. 1 Layout of the boreholes where seismic tests were performed

CH tests were performed on three dried out PVC cased boreholes, as shown in Fig. 1. Data acquisition took place between boreholes S2-S1, S3-S1 and S3-S2 defining three sections respectively 4.98 m, 3.64 m and 3.53 m wide, until to a maximum depth of 18 m. These tests were carried out in April and February, with the groundwater level estimated at around 4m depth.

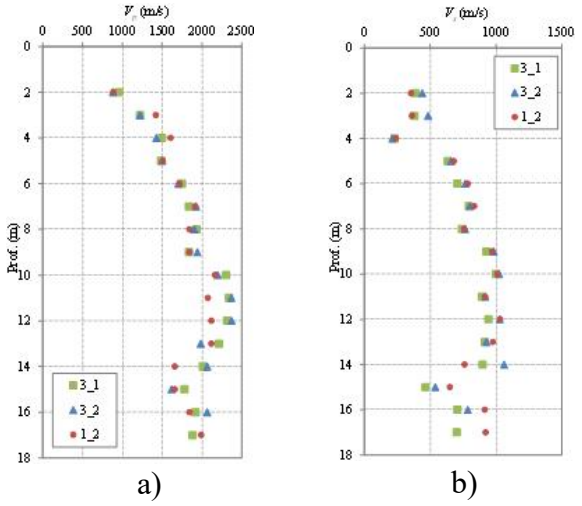

Fig. 2 Results from CH tests using a mechanical source: a) V_P; b) V_S

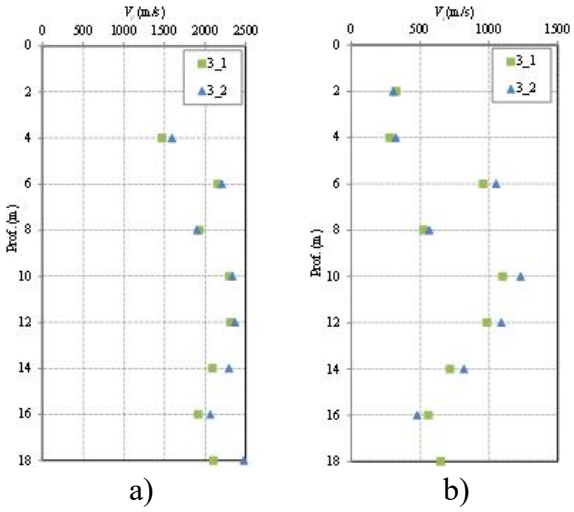

Fig. 3 Results from CH tests using a S-wave sparker source: a) V_P; b) V_S

Direct and derived results from the applied techniques were compared between them, as well as with some of the available geological and geotechnical information. S-waves and P-waves velocities, V_S and V_P, variability with depth can be seen in Fig. 2 and Fig. 3 corresponding to CH sections S2-S1, S3-S1 and S3-S2 with mechanical and sparker sources respectively. V_P profiles are very similar using the mechanical hammer and the sparker source. V_P varies between 1500 m/s and 2500 m/s, and is close to 1500 m/s at 4.0 m depth, which is consistent with the estimated position of the groundwater table. There is an increase in V_P between 6.0 m and 10.0 m depth, which is probably related to the passage from greenish clay to marly clay, reported in the borehole log, with a correspondent increase in SPT results. Results between different pairs of boreholes are quite alike, as it was expected to, given the proximity of the boreholes.

Regarding V_S, Fig. 2 and Fig.3 show the average values of the measurements in the three channels, with distinct orientations, which were very similar. The same situation occurred for the tests using a mechanical source, and these are also the average of values measured in different channels. These occurrences may have constrained the identification of the hypothetical diffuse clay anisotropic stress state based on S_{hv} and S_{hh} wave velocities.

Derived values of shear modulus, G_0, and Poisson's ratio, were estimated from seismic velocities. Poisson's ratio at 4.0 m depth is around 0.5 which is consistent with the assumed groundwater table position. Shear modulus is lower in the shallower layers and increases considerably between 9.0 m and 13.0 m depth, where a light grey marly clay with NSPT over 60 blows was identified.

Seismograms were treated and interpreted both in time, frequency and time-frequency domains. In time-frequency domain, in addition to the more conventional short-time Fourier transform, STFT, an innovative in this context use of the fast S-transform, FST, adapted from Stockwell et al [4], was carried out with significant improvements, namely in resolution gain in detecting and temporally localizing the different frequency wave packets, in particular related to P-waves and S-waves. The S-transform is basically a frequency dependent variable Gaussian window short time Fourier transform, as well as an extension of the wavelet transform.

The next six seismograms, S4N31 (1 2 3) and s247 (1 2 3), shown in Fig. 4a) and Fig. 4b), were obtained at 4 m depth, in a clay layer with N-SPT of 37, using a sparker source and a mechanical bidirectional vertical borehole hammer respectively. An initial significantly higher frequency and rather high amplitude wave trains, related basically to P-waves followed

by the S-wave train is very noticeable. For a more accurate assessment of the signal's frequency content related predominantly with P-waves and S-waves and their respective time location, magnitude Fourier transforms, and spectrograms based on Fourier transforms, STFT, and S-transforms, FST, will be shown next. Fig. 5 shows the magnitude Fourier transform of seismogram S4N31_1 being noticeable a 500 Hz - 1750 Hz significant frequency bandwidth.

Next, two spectrograms based on the more conventional STFT and another two on the frequency dependent variable Gaussian window S-transform, FST, are compared. Fig. 6 shows two variants of seismogram S4N31_1 STFT and Fig. 7 shows two variants of S4N31_1 FST spectrograms. In both spectrograms the one at the left side more frequency – time informative but showing less resolution concerning P-wave and S-wave packs distinction and time location.

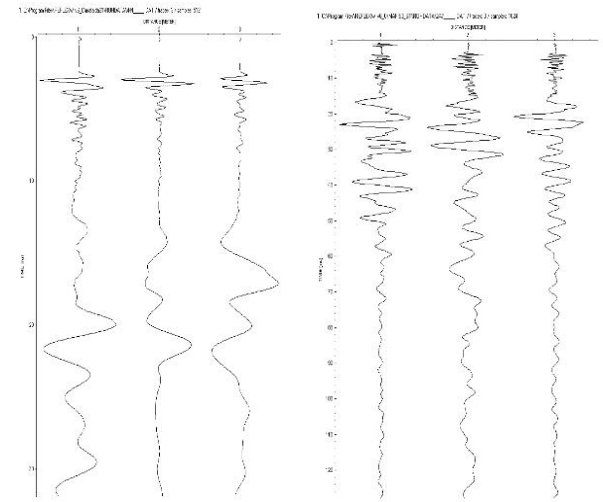

a) **b)**

Fig. 4 Seismograms S4N31 (1 2 3) and s247 (1 2 3)

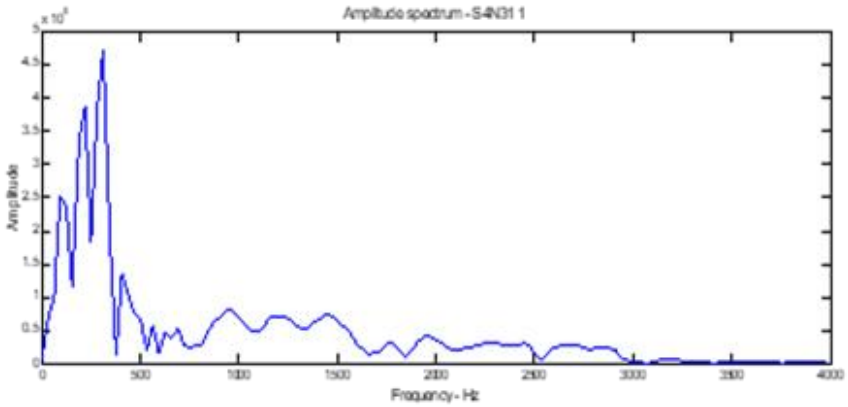

Fig. 5 Seismogram S4N31_1 magnitude Fourier transform

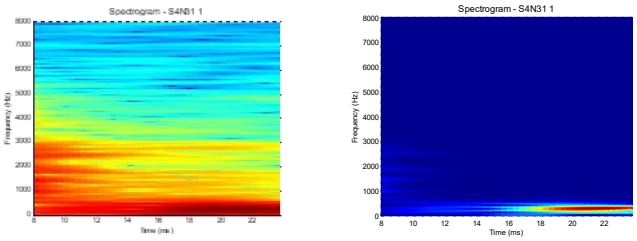

Fig. 6 Seismogram S4N31_1 STFT spectrograms

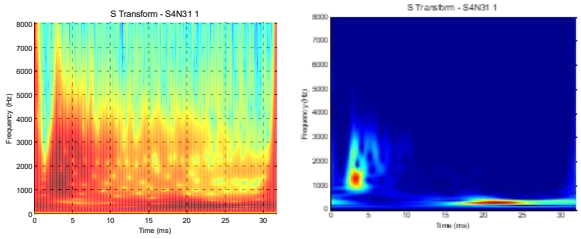

Fig. 7 Seismogram S4N31_1 FST spectrograms

The left side spectrogram in Fig. 7 shows distinctively the P-wave pack with a center frequency around 1250 Hz, followed by a higher partly noise frequency band. It is also possible to distinctively observe the vertically polarized S-wave pack with a center frequency around 270 Hz. The improvement in resolution when using the FST comparatively with the STFT is obvious and very significant. The FST allows a much clearer distinction between the first higher frequency P-wave pack and the following arrival of the S-wave pack. The advantage is significant not only in terms of the much clear wave packets location both in time and frequency domains, but also in terms of their relative associated amplitude.

Fig. 8 shows the z-geophone and y-geophone seismograms. As expected due to the type of sparker source, the P-wave and especially S-wave amplitudes are higher in the y-geophone.

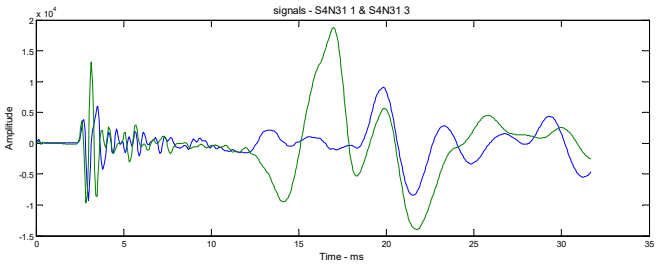

Fig.8 Seismograms S4N31_1 and S4N31_3

All the previous seismograms obtained at 4 m depth contain an initial very significant P-wave pack not visible in any of the seismograms obtained at 2 m depth. This kind of occurrence has been observed before [5, 6] and is interpreted as being related to the soil water content, in particular to the non-saturated and saturated soil horizons interface. Therefore, the sudden

occurrence of very distinct initial high frequency P-wave packs is interpreted as a sign of saturation. Coherent with this assumption is the fact that at 4 m depth P-wave velocities vary around 1500 m/s as it is shown in Fig. 3 and inversely at this depth, the S-wave decreases, probably due to a decrease in both the related soil suction effect and related shear strength.

Next examples refer to data collected with the vertical borehole hammer at 4 m depth. Generically and as in the previous seismograms at depth 4 m, the initial higher frequency P-wave train followed by the higher amplitude polarized S-wave trains is visible..

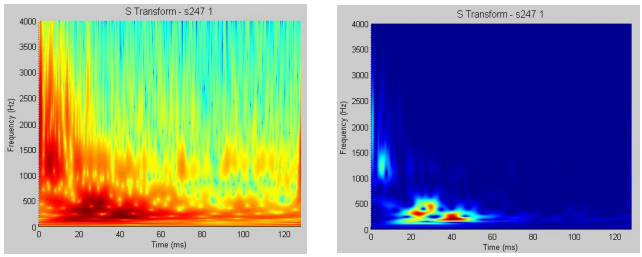

Fig. 9 Seismogram s247_1 magnitude Fourier transform

Fig. 9 shows the magnitude Fourier transform of seismogram s247_1 where predominant amplitudes at around 200 Hz and 320 Hz occur. Fig. 9 shows distinctively on the right side FST spectrogram the P-wave pack with a center frequency around 1250 Hz and two distinct S-wave trains with center frequencies around 300 Hz and 200 Hz, starting at 15 ms. and ending at around 60 ms.

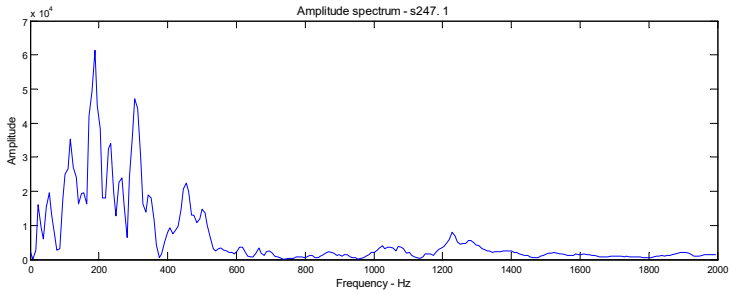

Fig. 10 Seismogram s247_1 FST spectrograms

Fig. 11 on the left side shows the magnitude Fourier transform of seismogram s247_2 with predominant amplitudes at around 50 Hz and at around 200 Hz, as in the previous case. Seismogram s247_2, Fig. 11, shows an initial higher frequency P-wave train followed by the lower frequency horizontally polarized S-wave train. Fig. 11 shows on the right-side seismogram s247_2 FST spectrogram showing an attenuated P-wave pack with a center frequency around 1250 Hz. It is also possible to observe, although less distinctively than in

the z-geophone, the horizontally polarized S-wave pack. Generically and comparatively with the previous case there is a S-wave pack less intense and spreading less in frequency.

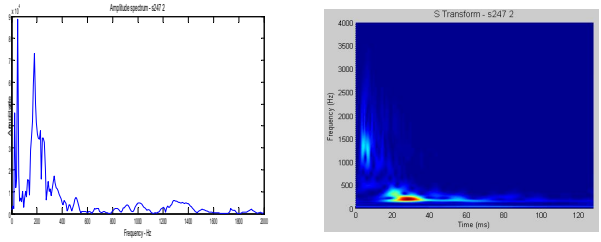

Fig 11. Seismogram s247_2 magnitude Fourier transform and FST spectrograms S

Fig. 12 shows the z-geophone s247_1 and x-geophone s247_2 seismograms. The P-wave and S-wave amplitudes are rather similar in both seismograms. The s247_3 seismogram, Fig.13, has an initial higher frequency P-wave train followed by the lower frequency horizontally polarized S-wave train but, comparatively with s247_2 seismogram, has higher P-wave and S-wave amplitudes. This fact suggests that the horizontal geophones were not orthogonally and collinearly oriented as it was supposed. Fig. 13 shows on the left side the magnitude Fourier transform of seismogram s247_3 being noticeable predominant amplitudes up to around 500 Hz and on the right side seismogram s247_3 FST spectrogram having a P-wave pack with a center frequency around 1250 Hz. It is also possible to observe the horizontally polarized S-wave pack more distinctively than in the previous case.

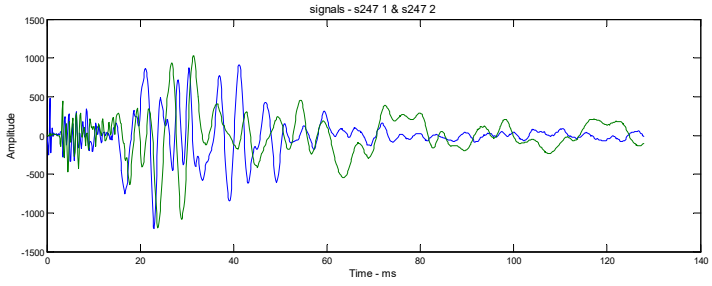

Fig 12. Seismograms s247_1 and s247_2

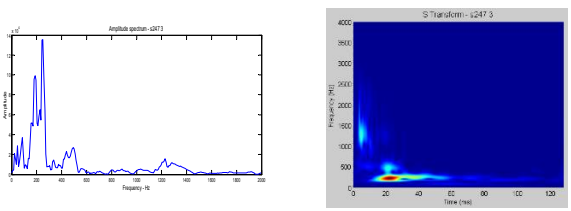

Fig 13. Seismogram s247_3 magnitude Fourier transform and FST spectrograms.

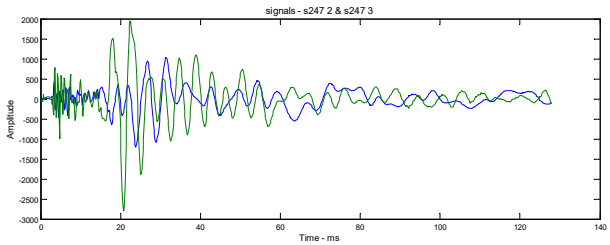

Fig 14. Seismograms s247_2 and s247_3.

Fig. 14 shows the x-geophone s247_2 and y-geophone s247_3 seismograms having the second one higher amplitude especially for the S-waves train. Unexpectedly, due to the vertical hammer source designed to generate vertically polarized S-waves, it is the s247_3 seismogram that has larger amplitudes quantified by a much larger normalized total energy and normalized summation, when compared with the other two seismograms, s247_1 and s247_2. No reasonable explanation has been found, so far, for such occurrence.

4.2 Mechanical tests

In spite of the natural spatial variability of these soils, there is evidence of a fairly homogeneous ground profile in geotechnical terms. The site characterization mechanical tests included SPT along borehole 1, 4 Menard pressuremeter tests, PMT, along borehole 3 and 3 self-boring pressuremeter tests, SBPT, along borehole 2.

Miocene formation was identified from 3.0 m depth, and most soils are clays an marly clays with some calcareous intercalations between 10.5 m and 13.5 m depth. N_{SPT} is over 60 blows from 4.5 m depth and there is a stiffer layer of soil between 6.0 m and 12.0 m where 60 blows were achieved during the first increment.

PMT tests were performed at 4 depths along borehole 3 using a 60 mm diameter probe which corresponds to a maximum injection volume of 750 cm^3. From these four PMT tests, only S3-01, at 15.5 m depth, showed a typical S curve. Tests S3-02, at 13.0 m depth and S3-03 at 7.5 m depth, showed no inflection of the curve after the maximum volume was injected, so the obtained p_0 value is actually the lower limit of p_0. E_M/p_0 ratio corresponds to hard to very hard soils, [7] and derived undrained shear strength (s_u) varies between 250 kPa and 310 kPa [8, 9].

SBPT tests were performed at 3 different depths along borehole 2, namely 4.75 m (T1), 9.5 m (T2) e 15.5 m (T3). The equipment comprised six extensometers, its maximum working pressure was 10 MPa, and a stiffer than usual membrane was used. The outer diameter of the probe was 87 mm and the diameter of the rock roller bit was 73 mm. The length of sacrificed soil was of 1.0 m to 1.5 m at each tested depth. The lift-off pressure was derived from the

expansion curves allowing estimating the earth pressure coefficient at rest, K_0, assuming ground water level at 4.0 m depth. Undrained shear strength, s_u, was determined using different approaches [10, 11]. T1 and T2 allowed estimating s_u equal to 229 kPa and 1116 kPa, respectively, and limit pressure values of 1315 kPa and 4491 kPa.

Regarding the shear modulus, G, the obtained values from these tests are lower than those commonly reported for *Prazeres* clay formation. This fact may be related and explained by the lower confining pressures prevailing at the investigated site. Undrained shear strength, s_u, is consistent with the commonly reported for this formation although the differences observed between the peak and residual values based on Palmer analysis are more expressive than those previously observed and reported.

5 Laboratory tests on undisturbed samples

5.1 Testing equipment and materials

The laboratory geophysical testing on intact samples was performed by means of bender elements, either on the workbench, prior to the assemblage of triaxial tests, or in triaxial chambers that have been adapted accordingly [12]. Shear wave velocity measurements were also performed on the workbench using the ultrasonic transducers of Pundit® equipment [13]. The bender elements equipment comprises a function generator (TTi 110), which can generate an electric signal with different configurations. In the present work the sinusoidal configuration was used for different frequencies, which were adapted based on the quality of the received signal. The viewing and acquisition of both emitted and received signals is possible through a Tektronix® oscilloscope TDS220.

Pundit® equipment allows generating signals with steady frequencies and is connected to a computer that records the signals emitted and received by two ultrasonic transducers. One of the advantages of its use compared to bender elements is that the shear wave is emitted through contact with the soil specimen, and there is no need of penetrating the sample, unlike what happens with bender elements. When high consistency soils are being tested, the bender's penetration can be accompanied by cracks on the sample, thus compromising subsequent tests.

With this equipment, only P-wave measurements were carried out prior to the assemblage of triaxial tests. S-wave velocities were not successfully measured as the available frequencies

have proved to be too high. This has shown to be a limitation of this equipment, since the available frequencies are discrete and steady, with a minimum central value of 24 kHz, which is considerably higher than the maximum emitted central signal frequency with bender elements to measure S-waves that was of 8 kHz [14]. Fig. 15 shows some aspects of these measurements.

a) b) c)

Fig. 15 Some aspects of the measurement of seismic wave velocities with Pundit® equipment: a) test setting; b) P-wave measurement; c) S-wave measurement

5.2 Compression and shear waves velocity measurements

Shear modulus and Poisson's ratio were derived from S and P-wave velocity measurements. A total of 6 samples were tested on the workbench, prior to its placement in the triaxial cell, and these measurements were compared with in situ seismic CH measurements at 4.0 m depth, in order to assess the quality of the sampling. When adapted to accommodate bender elements triaxial cells were used, the seismic wave velocity measurements were performed in different phases of the test, namely the end of saturation, end of consolidation and shear for different deformation levels. The results obtained from bender element measurements are summarized in Table 1 and Table 2, concerning measurements on the workbench and results obtained during triaxial tests respectively.

Table 1 Shear modulus, Poisson's ratio and Young modulus from bender elements measurements

Sample #	G_0 (MPa)	$_{din}$	E_0 (MPa)
in situ (4,0 m depth)	149.73	0.48	444.04
Sample 5	28.05	0.47	82.45
Sample 6	38.48	0.47	103.51
Sample 7	50.75	(1)	(1)

Sample 9	107.98	(1)	(1)
Sample 10	33.41	0.48	99.15

Table 2 Shear modulus, Poisson's ratio and Young modulus from bender elements measurements during triaxial tests

Sample #	Phase	G_0 (MPa)	$_{din}$	E_0 (MPa)
5	End saturation	21.74	0.50	65.12
	End isotropic consolidation	39.71	0.50	87.46
	End anisotropic consolidation (K0=1.2)	31.58	0.50	458.61
6	End saturation	31.58	0.50	94.53
	End isotropic consolidation	154.25	0.49	458.61
10	End saturation	32.36	0.50	96.88
	End isotropic consolidation	40.60	0.50	121.47

A first glance at the results from Table 1 suggests that there is a very good agreement between the values measured for all samples, and these are considerably lower than the values measured in situ, from CH tests at the correspondent depth. The average values obtained were 48.7 (±27.4) MPa for G_0 and 98.4 (±12.7) MPa for E_0. The average Poisson's ratio of 0.47 (±0.005) is consistent with what is expected for saturated soils. Another interesting aspect is the evolution of G_0 from the workbench, at the end of saturation and the end of consolidation. A comparison between Table 1 and Table 1 shows that G_0 and E_0 slightly decrease from the workbench to the end of saturation, and this can compromise the repeatability of these results. It is worth pointing out that the main differences measured were in the P-wave velocities as S-wave did not show considerable variations.

Table 2 allows verifying that during consolidation, as the confining stress increases G_0 also tends to increase. Actually, it is possible to state that S-wave measurements are very sensitive to confining stresses. All the studied samples have shown an increase in G_0, and this was more significant in sample 6, which had the higher confining stress ($'_c$ = 600 kPa). Samples 5 and 10 were consolidated to the same stress ($'_c$ = 80 kPa), and the obtained values are alike.

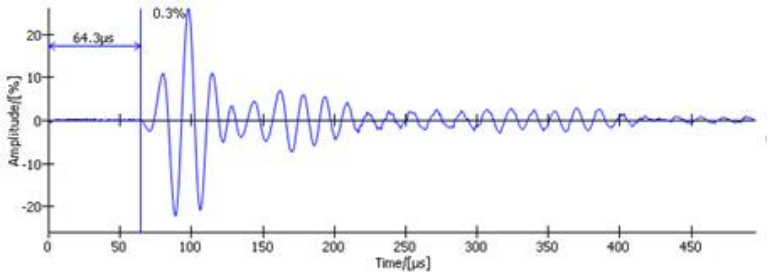

Fig. 16 P-wave velocity measurement with ultrasonic transducers in sample 5 Pundit® (82 kHz)

CH in situ measurements at 4,0 m depth were compared with results for sample 5, as this sample was tested in conditions considered representative of the in-situ stress state. It is possible to observe that the laboratory measurements are considerably lower than the 149.73 MPa obtained in field measurements, despite all the caution during block sampling and subsampling prior to triaxial tests. Thus, the stress state changes due to decompression are not to be neglected. From all measurements performed with ultrasonic transducers only P-wave propagation velocity measurements on sample 5, which was of 1574.5 m/s as shown in Fig. 16 were considered reliable. For the other samples the received signals were not clear enough to allow identifying the P-waves arrival time.

6. Discussion – correlations and trends

G_0 shear strength values derived from laboratory seismic wave velocity measurements were around 26 % of the obtained in the field, which is understandable and expected due basically to the sampling decompression effect. Stiffness degradation was evaluated during triaxial tests yield phase using internal measuring devices. Table 3 shows initial and secant stiffness values measured for extensions of 0.01 %, 0.1 %, 0.5 % and 1.0 %. Besides stiffness degradation with extension, it was observed a stiffness increase with increasing confinement stress. Since these triaxial tests were performed in a high-pressure chamber, confinement stresses are significantly higher than in situ stresses, so comparing these E values with E_0 obtained in situ should be done with caution.

Table 3 Table 3. Stiffness measured for different extensions measured in triaxial tests on intact *Prazeres* clay samples

Test	E_i (MPa)	$E_{0,01\%}$ (MPa)	$E_{0,1\%}$ (MPa)	$E_{0,5\%}$ (MPa)	$E_{1,0\%}$ (MPa)
$'_c$= 1000 kPa	1772	-	429	133	86

’$_c$= 4150 kPa	954	-	872	367	227
’$_c$= 6500 kPa	8295	6622	2609	804	534
’$_c$= 9100 kPa	3781	-	2507	1092	650

Fig. 17 shows E_{sec} / E_i for every loading stage as a function of stress level (SL), defined as the incremental shear strength divided by shear strength at failure. A significant decrease in stiffness while increasing the stress level, SL is possible to observe. For SL near unity the ratio E_{sec} / E_i tends to vanish. It was verified that as well as with the shear strength the initial secant Young modulus is significantly lower than those obtained with bender elements.

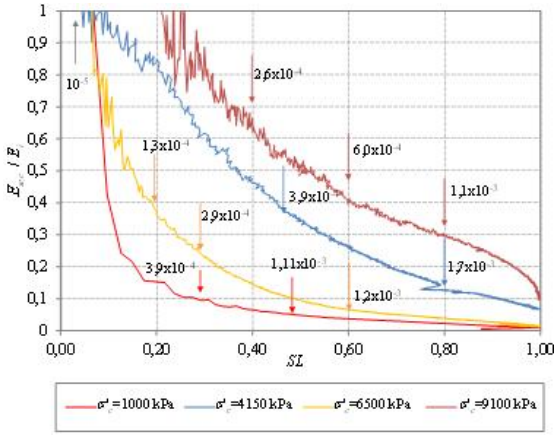

Fig. 17 E_{sec} / E_i in triaxial compression tests.

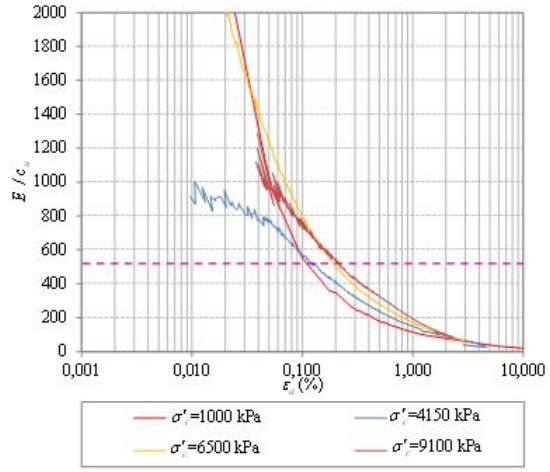

Fig. 18 E / s_u in triaxial compression tests

Fig. 18 shows E_{sec} / s_u variation with extension. It is possible to observe that all curves plot in a relatively narrow band, meaning that this ratio is not dependent on consolidation stress. The same figure shows proportionality parameter M equal to 520 as described in the literature [15], meaning there is a good agreement between these results and PMT parameter for axial extensions between 0.1 % and 0.2 %.

The combined analysis of the field testes carried on at the experimental site in Av. Visconde Valmor in Lisbon, allows various considerations regarding the stiffness and deformability characteristics of *Prazeres* clay formation.

Although shear modulus values obtained with seismic cross-hole and pressuremeter tests are rather different in both results is noticeable a coincident tendency for an increase in stiffness between depths 8,0 m and 14,0 m in accordance with SPT results. It was observed that stiffness parameters evolve according to the expected tendency: G_0 (CHT) > Gi (SBPT) > G_M (PMT) [14].

7. Conclusions

In situ seismic cross-hole tests were performed during two campaigns using different equipment, particularly two seismic sources, a mechanical bidirectional hammer and an S-wave sparker probe. It was then possible to compare seismic signals obtained with the referred equipment. Also, subsequently to an initial more conventional frequency domain analysis using the Fourier transform the short-time Fourier transform, was used and compared with the S-transform in terms of their relative time/frequency domains resolution.

Concerning the referred two seismic sources, it was observed that the sparker probe was very efficient in generating clearly detectable P-waves often in the three orthogonally oriented geophones although less accurate regarding the polarity orientation of the S-waves at the shot-point.

The time/frequency domain analysis clearly showed a very significant improvement in frequency resolution and time positioning of the P-wave and S-waves signal components when using the S-transform approach comparatively with de short-time Fourier transform. The use of the S-transform combined with the median frequency, normalized total energy and normalized summation, allowed a better understanding of the seismic signals and their generation and reception conditions, optimizing consequently their interpretation.

Worth mentioning again the suction effect above the groundwater level in the variability of the S-waves velocity vertical profiles, when passing from the unsaturated to the saturated horizons, due to an associated increase of rigidity. Also, at these transition depths it has been observed the occurrence of very significant around 1500 m/s P-wave packets, not visible in any of the seismograms obtained above the saturated horizon.

Cross-hole seismic tests provide significantly higher stiffness G_0 values. PMT test results were fit for this type of clay formation, and stiffness degradation with extension is very noticeable. Seismic tests performed in the laboratory allowed to control stiffness degradation during triaxial tests and to establish a constant E_u / s_u value which can be useful for geotechnical design.

Acknowledgement

This paper was developed within the PTDC/ECM/64167/2006 research project, and within the scope of the project proMetheus – Research Unit on Materials, Energy and Environment for Sustainability, FCT, Ref. UID/05975/2020, financed by national funds through the FCT/MCTES.

References

[1] Antunes, M. T., P. Legoinha, P. P. Cunha and J. Pais. "High resolution stratigraphy and miocene facies correlation in Lisbon and Setúbal Peninsula (Lower Tagus basin, Portugal)." Ciências da Terra (UNL) 14: 183-190, 2000.

[2] Zbyszewski, G. "Panorama sur la Geologie de la Ville de Lisbonne." Boletim da Sociedade de Geografia de Lisboa 65, Série (9-10), 1947.

[3] Moitinho de Almeida, F. "Carta Geológica do Concelho de Lisboa". S. G. d. Portugal, Serviços Geológicos de Portugal, 1986.

[4] Stockwell et all. "Localization of the complex spectrum: the S transform". IEEE Trans Signal Process 44: 998-1001, 1996, DOI: 10.1109/78.492555.

[5] Carvalho, J., Fonseca, A.V., Almeida, F., Hermosilha, H. "ISC'2 experimental site investigation and characterization – Part I: conventional and tomographic P and S waves refraction seismics vs. electrical resistivity". Geotechnical and Geophysical Site Characterization, Proceedings of the 2nd International Conference on Site Characterization, ISC-2", Porto, Portugal, 19-22 September 2004, Viana da Fonseca & Mayne (eds), 2004 Millpress, Rotterdam, ISBN 90 5966 009 9 (pgs. 1361-1369, (pp. 433-441).

[6] Viana da F. A; Carvalho, J.; Ferreira, C.; Santos, J. A; Almeida, F.; Pereira, E.; Feliciano, J.; Grade, J.; Oliveira, A. "Characterization of a profile of residual soil from granite combining geological, geophysical and mechanical testing techniques". Geotechnical and

Geological Engineering V24, Nº 5: pp. 1307-1348. (ISSN: 0960-3182, Print, pp.1573-1529, Online).doi: 10.1007/s10706-005-2023-z. ICDS = 10.0.Viana et al., 2006

[7] Clarke, G. B., Ed. "Pressuremeters in geotechnical design". London, Chapman and Hall, 1995.

[8] Cassan, M. "2Les Essais in situ em Méchanique des Sols. Tome 1: Realization et Interpretation". E. Eyrolles. Paris, Editions Eyrolles, 1978.

[9] Briaud, J. L. "The pressuremeter". Rotterdam, Netherlands, A.A. Balkema, 1992.

[10] Gibson, R. E. and W. F. Anderson. "In situ measurements of soil properties with the pressuremeter." Civil Engineering and Public Works Review 56(658): 615-618, 1961.

[11] Palmer, A. C. "Undrained plane-strain expansion of a cylindrical cavity in clay: a simple interpretation of the pressuremeter test." Géotechnique 22(3): 451-457, 1972.

[12] Ferreira, C. "The Use of Seismic Wave Velocities in the Measurement of Stiffness of a Residual Soil". Civil Engineering, Porto, Porto. PhD Thesis, 2009.

[13] Tallavó, F., G. Cascante and M. D. Pandey. "New Methodology for Source Characterization in Pulse Velocity Testing." Geotechnical Testing Journal 32(6), 2009.

[14] Lopes Laranjo, M. "Argilas Miocénicas de Lisboa. Parametrização para o Dimensionamento de Estruturas Geotécnicas". Civil Engineering, Porto, Porto. PhD Thesis, 2013.